# Selection and Amplification of Mixed-Metal Porphyrin Cages from Dynamic Combinatorial Libraries

**Eugen Stulz,*[a] Sonya M. Scott,[b] Andrew D. Bond,[c] Simon J. Teat,[d] and Jeremy K. M. Sanders*[b]**

**Abstract:** Mixed metallo–porphyrin cages were selected and amplified from dynamic combinatorial libraries (DCLs) by using appropriate templates. The cages are composed of two bisphosphine substituted zinc(II) porphyrins as ligand donors and two rhodium(III) or ruthenium(II) porphyrins as ligand acceptors, and are connected through metal–phosphorus coordination. Ru and Rh porphyrins that display a large structural diversity were employed. The templating was achieved by using 4,4′-bpy, 3,3′-dimethyl-4,4′-bipyridine and benzo[*lmn*]-3,8-phenanthroline, and acts through zinc–nitrogen coordination. The absolute amount of amplification from the DCLs is strongly dependent on the combination of the Ru/Rh porphyrin and the template; cages with sterically demanding porphyrins can only form with smaller templates. In the case of *tert*-butyl-substituted TPP (TPP = tetraphenylporphyrin), cages are not formed at all. The formation of the cages is usually complete within 24 h at an ambient temperature; in the case of the cage containing $Rh^{III}$OEP (OEP = octaethylporphyrin) and bpy, the pseudo-first-order rate constant of cage formation was determined to be $2.1 \pm 0.1 \times 10^{-4}\ s^{-1}$ ($CDCl_3$, 25 °C). Alternatively, heating the mixtures to 65 °C and cooling to room temperature yields the cages within minutes. The $^1H$ NMR chemical shifts of several characteristic protons show large differences upon changing the identity of the Ru/Rh porphyrin and the central metal; this is most likely to arise from variations in the geometry of the cages. The X-ray crystal structure of a cage, which contains $Rh^{III}$OEP as a porphyrin acceptor and bpy as template, demonstrates that the cages can adopt severely distorted conformations to accommodate the relatively short templates. An extension to mixed DCLs showed that only limited selectivity is displayed by the various templates. Formation of mixed cages that contain two different rhodium porphyrins prevents effective selection, although the kinetic lability of the systems allows for some amplification. This lability, however, also prevents isolation of the individual cages. Removal of the template leads to re-equilibration, thus the templates act as scaffolds to keep the structures intact.

**Keywords:** cage compounds · dynamic combinatorial libraries · phosphane ligands · porphyrinoids · self assembly

## Introduction

The study of dynamic combinatorial libraries (DCLs), and the selective amplification of species complementary to templates is a rapidly growing field of research.[1] The main difference from classical combinatorial libraries is the use of reversible bond formation, such that individual library members are interconverting at thermodynamic equilibrium. The technique creates large libraries of possible receptor compounds, and a template may be used to screen for its optimal receptor through a best-fit selection process. While the remaining library members are kinetically labile and interconverting under given experimental conditions, the target receptor will be thermodynamically stabilized as a non-covalent complex with the template. Thus the target receptor will be amplified, and in the best case, the whole library will be transformed to one specific molecule. DCLs have been prepared by using a variety of reversible bond formation

[a] Dr. E. Stulz
Department of Chemistry, University of Basel
St. Johanns-Ring 19, 4056 Basel (Switzerland)
Fax: (+41) 61-267-0976
E-mail: Eugen.stulz@unibas.ch

[b] Prof. J. K. M. Sanders, Dr. S. M. Scott
University Chemical Laboratory, University of Cambridge
Lensfield Road, Cambridge, CB2 1EW (UK)
Fax: (+44) 1223-33-60-17
E-mail: jkms@cam.ac.uk

[c] Dr. A. D. Bond
Syddansk Universitet, Kemisk Institut
Campusvej 55, 5230 Odense M (Denmark)

[d] Dr. S. J. Teat
CLRC Daresbury Laboratory, Warrington
Cheshire, WA4 4AD (UK)

Supporting information for this article is available on the WWW under http://www.chemeurj.org/ or from the author. This includes $^1H$ NMR analysis of mixtures 2 and 4, and the kinetic evaluation of the formation of cage **1**.

 DOI: 10.1002/chem.200305265  

processes, that include covalent,[2] non-covalent hydrogen-bonding,[3] and metal–ligand exchange.[4] Much of conventional coordination chemistry that leads to the formation of a dominant product could retrospectively be thought of as dynamic combinatorial, with the corresponding metal ion acting as a template. DCLs formed through metal–ligand coordination encompass a large range of systems with kinetically labile metal-complexes, and are of particular interest for the formation of supramolecular systems which might have useful redox or magnetic properties. A variety of different systems have been explored to date, for example, $Co^{II}$–terpy complexes,[4g] $Pd^{II}$–pyridine complexes,[4f] and $Ga^{III}$– or $Zn^{II}$–hydroxyquinoline complexes.[4d] These systems have generally utilized metal ions or organic molecules as the guest, and form the target complex through ionic interactions. Combination of metal–ligand and π–π interactions have been used to form crown ethers.[4h]

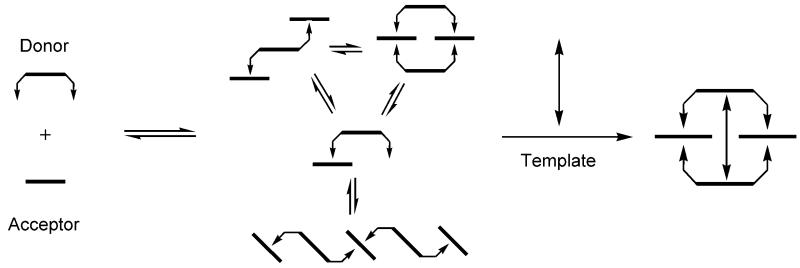


Scheme 1. Schematic representation of the DCL formation and templating of the cage. Arrowheads represent the ligands (P, N) to the central metal of the porphyrins (bars).

In the system described here, reversible metal–ligand binding is used for two roles simultaneously, both to form the DCL and for templating. The concept is applied to generate mixed-metal porphyrin cages selectively, and virtually completely, from DCLs. This study is a continuation of our earlier work,[5] in which we prepared a tetraporphyrin cage composed of two bisphosphine-substituted $Zn^{II}$ porphyrins as donors, two $Rh^{III}$TPPs as phosphine acceptors, and one 4,4′-bpy as a template (ligand), the cage being stabilized through orthogonal $Zn^{II}$–nitrogen and $Rh^{III}$–phosphorus coordination modes (Scheme 1). We now extend the study to include several different $Rh^{III}$/$Ru^{II}$ porphyrins and different templates, and also to combine $Rh^{III}$ or $Ru^{II}$ porphyrin building blocks in complex mixtures to examine the prospects for selective templating of new mixed-metal porphyrin cages (Table 1)

From previous studies on phosphorus[6,7] and nitrogen[5,8] complexes with metallo porphyrins, we know that the Ru/Rh–P bond is kinetically more inert than the Zn–N bond. This is manifested in, for example, the $^1$H NMR spectrum for bpy bound to zinc porphyrin: the resonances appear broad, and the chemical shift is concentration dependent, which indicates fast exchange between free and bound species. The first binding constant of bpy to ZnTPP is $6\times 10^3\,\text{M}^{-1}$.[5] For phosphines bound to rhodium or ruthenium porphyrins with a binding constant in the range of $10^6$ to $10^7\,\text{M}^{-1}$,[6,7] the resonances are generally sharp and well resolved, which indicates slow ligand exchange. These values were determined by using a model ligand, diphenyl(phenylacetenyl)phosphine (DPAP), that has an identical substitution pattern on the phosphorus but does not possess the porphyrin moiety. In the DCLs, which are prepared at the millimolar concentration level, most of the Ru/Rh sites will therefore be complexed by phosphine ligands. Despite the lability of the Zn–N bond, formation of the cage traps the template in a two point binding mode, thus increasing the thermodynamic stability by a chelate effect, and allowing for amplification.

Table 1. Composition of the cages.

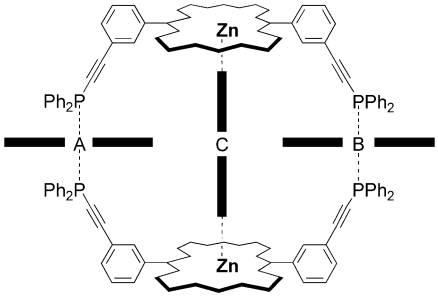


| Cage | A | B | C |
|---|---|---|---|
| 1 | Rh**2** | Rh**2** | bpy |
| 2 | Rh**3** | Rh**3** | bpy |
| 3 | Rh**4** | Rh**4** | bpy |
| 4 | Ru**2** | Ru**2** | bpy |
| 5 | Ru**3** | Ru**3** | bpy |
| 6 | Ru**4** | Ru**4** | bpy |
| 7 | Rh/Ru**5** | Rh/Ru**5** | bpy |
| 8 | Rh**2** | Rh**2** | **6** |
| 9 | Rh**2** | Rh**2** | **7** |
| 10 | Rh**3** | Rh**3** | **6** |
| 11 | Rh**3** | Rh**3** | **7** |
| 12 | Rh**3** | Rh**2** | bpy |
| 13 | Rh**3** | Rh**2** | **6** |

## Results and Discussion

**Structural diversity in the acceptor porphyrin**: To examine the steric influence of substituents on the acceptor porphyrin, we investigated the ability of four rhodium porphyrins Rh**2**–Rh**5**, and four ruthenium porphyrins Ru**2**–Ru**5**, to form cages, as shown in Scheme 2. The composition and numbering of the cages formed throughout the study is also displayed, and Table 2 gives selected relevant NMR data which are discussed below. $^1$H NMR studies on equimolar mixtures of Zn**1** with each of the acceptor porphyrins prior to addition of bpy showed the formation of dynamic combinatorial libraries containing numerous complexes.[5] Titration of one equivalent of bpy into the mixtures followed by annealing (see Experimental Section) resulted in the series of spectra shown in Figure 1. The sharp and well resolved signals of the spectra in Figure 1b–g suggest that a single

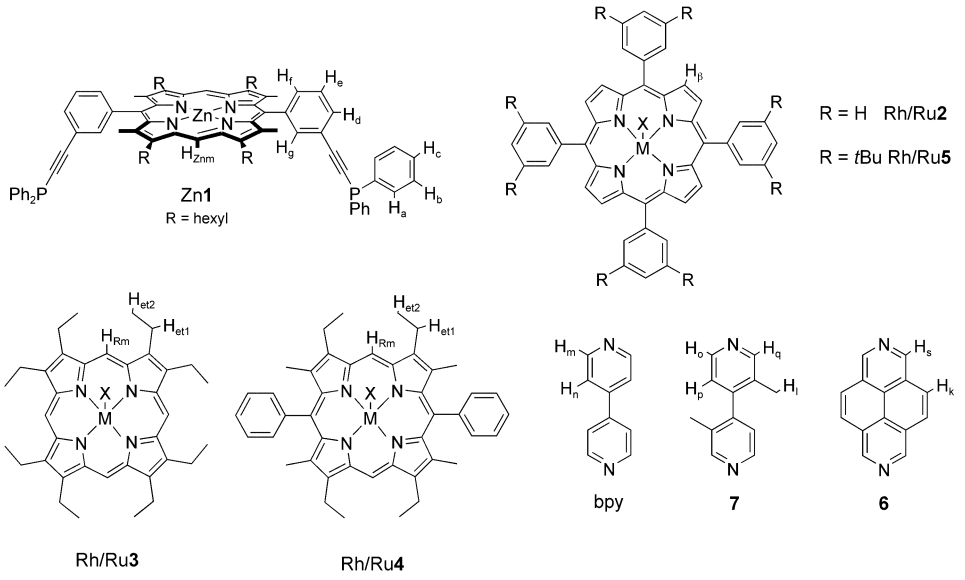


Scheme 2. Porphyrin and template structures with key protons labeled. For the rhodium porphyrins, M–X = $Rh^{III}$–I; for the ruthenium porphyrins, M–X = $Ru^{II}$–CO.

Table 2. $^1$H NMR data [$\delta$] of the cages. The labeling of the resonances is in accordance with Scheme 2.

| | cage **1** | cage **2** | cage **3** | cage **5** | cage **6** | cage **7** | cage **8** | cage **9** | cage **10** | cage **11** |
|---|---|---|---|---|---|---|---|---|---|---|
| Znm | 10.05 | 10.16 | 10.21 | 9.98 | 10.08 | 10.10 | 10.11 | 10.11 | 10.28 | 10.12 |
| Rm/Rβ | 8.68 | 9.68 | 9.84 | 8.05 | 8.86 | 9.11 | 8.60 | 8.60 | 9.54 | 9.70 |
| a | 4.2 | 3.86 | 4.07 | 4.62 | 4.23 | 4.44 | 4.18 | 4.18, 3.94 | 3.78 | 3.84 |
| b | 6.62 | 6.43 | 6.53 | 6.51 | 6.34 | 6.43 | 6.65 | 6.72, 6.44 | 6.39 | 6.41 |
| c | 7.05 | 6.9 | 6.96 | 6.79 | 6.67 | 6.72 | 7.06 | 7.09, 6.98 | 6.87 | 6.88 |
| f | 8.07 | 8.19 | 8.19 | 7.93 | 7.99 | 7.98 | 8.00 | 8.14 | 8.18 | 8.22 |
| g | 7.82 | 7.47 | 7.44 | 8.05 | 7.55 | 7.58 | n.d.[a] | n.d.[a] | 6.61 | 7.53 |
| l | | | | | | | | −0.17 | | 0.27 |
| m | 2.14 | 2.45 | 2.40 | 2.01 | 2.32 | 2.27 | | | | |
| n | 4.49 | 5.43 | 4.87 | 4.09 | 5.13 | 4.73 | | | | |
| o | | | | | | | | 1.83 | | n.d.[a] |
| p | | | | | | | | 3.54 | | 4.77 |
| q | | | | | | | | 1.91 | | n.d.[a] |
| r | | | | | | | 2.94 | | 3.20 | |
| s | | | | | | | n.d.[a] | | 2.45 | |

[a] n.d. = not detected.

cage structure (cage **1** to cage **6**) templated by bpy is formed in each case. On addition of bpy to the DCL that contain the more sterically hindered Ru**5** or Rh**5**, the NMR spectrum (Figure 1a) remains complex, which implies that these systems still exist as mixtures of various compounds, and that no templating effect occurs. Thus with neither ruthenium nor rhodium porphyrins, cage **7** does seem to be accessible in this way. Titration of excess pyridine into the solution that contains the amplified cage **1** (with a heating-cooling annealing procedure performed after every addition) revealed that 50 equivalents of pyridine were required to reduce the amount of cage present by 40%; this suggests that the cage displays significant stability.[5] The preparation of ruthenium porphyrin cages was more complex due to the presence of the carbonyl group, which had to be removed prior to the formation of the cage by repeated dissolving/evaporating of the ruthenium porphyrin phosphine mixture.[9]

The cages formed were also characterized by two dimensional $^1$H NMR spectroscopy. Figure 2 shows a selected region of the $^1$H$^1$H NOESY spectrum of cage **2** as a representative example. NOEs are observed from the bpy protons ($H_m$ and $H_n$) to the ethyl sidechain protons on the OEP porphyrins ($H_{et1}$ and $H_{et2}$), and also from $H_g$ of the donor porphyrin (Zn**1**) to $H_{et1}$ of the acceptor porphyrin (Rh**3**). Combined with the upfield shifted resonances of the bpy signals ($H_m$ and $H_n$, see Table 2), this confirms that the final complex formed does have a cage-type structure, as depicted.[5] A broad peak at 2.48 ppm in the spectrum of cage **2** showed NOEs to most of the protons except $H_m$ and $H_n$ of the bpy (dashed line in Figure 2). After adding the rhodium porphyrin as MeOH-solvate, this signal almost certainly represented displaced methanol from the rhodium, which in this case, is preferentially absorbed within the cage. This was not observed for any other cage.

NMR studies on cages **1**–**6** show that the chemical shifts of most protons are independent of the identity of the porphyrin acceptor. However, a few specific protons are influenced by the overall composition of the cage (Table 2). For the Rh porphyrins, the proton $H_g$, which is pointing into the cages, is more deshielded in cage **1** ($\delta$ = 7.82 ppm) than in cage **2** ($\delta$ = 7.47 ppm) or cage **3** ($\delta$ = 7.44 ppm). The Ru porphyrins show an analogous trend, except that all protons are deshielded by 0.2 ppm compared with their Rh counterparts. The changes in chemical shift for the different acceptor porphyrins can be attributed to the overall geometry of the cage, the geometries of cage **2**, cage **3**, cage **5**, and cage **6** are similar, while the more sterically restricted cage **1** and cage **4** might adopt different conformations. In the latter two cages, $H_g$ is located in an overall less shielded region. The proton $H_f$, which is located on the outside of the cage, shows the opposite trend but with smaller $\delta$ values. The Ar–C≡C–P–M–P–C≡C–Ar unit must be sufficiently flexible to allow twisted conformations, as suggested previously.[5] This conclusion is also confirmed by the X-ray crystal structure determination of cage **3** (see below). In all cages, the effective symmetry of the Rh or Ru porphyrin is retained in solution

  

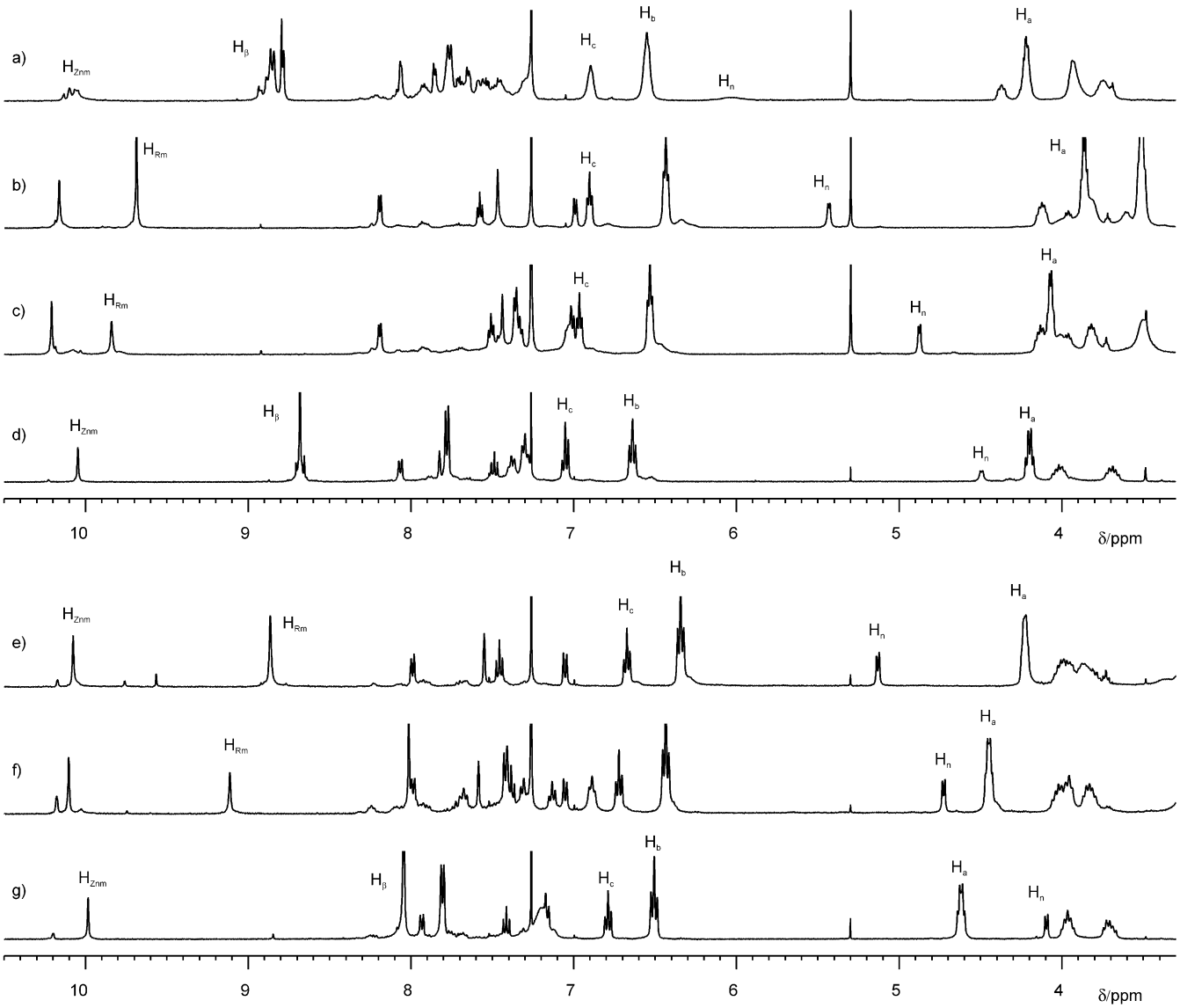


Figure 1. $^1$H NMR spectra of the amplification of the cages from the DCLs: a) cage **7**(Rh), b) cage **2**, c) cage **3**, d) cage **1**, e) cage **5**, f) cage **6**, g) cage **4**. Key resonances are labeled according to key protons of the porphyrins.

with a single resonance for each type of proton; this indicates rapid rotation about the P–M bond. Thus, the resonances observed reflect an average value for the protons located on the interior and on the outside of the cage.

The chemical shifts of the protons for the phosphine phenyl substituents are noteworthy. These protons undergo characteristic upfield shifts on binding to the Rh/Ru porphyrins, with the largest shift observed for $H_a$, the proton closest to the shielding region of the porphyrin. Similar shifts are observed for model complexes of the Ru and Rh porphyrins with DPAP.[6,7,10] $H_a$ occurs in the most upfield position in cage **2**, whereas in the cages **1** and **3** the downfield shifts are slightly smaller. $H_b$ shows a similar trend but with a smaller shift differences between the various cages, and $H_c$ resonates at approximately the same value for all cages. The signals for the protons $H_a$, $H_b$ and $H_c$ for cage **1** and cage **4** are shown in Figure 3. The $^1$H NMR data (Table 2) show that the chemical shifts of analogous protons between the same cages but with different metals, for example, in cage **1** (Rh) vs cage **4** (Ru), vary by about 0.5 ppm for $H_a$. An X-ray crystallographic study on model complexes of DPAP with all the acceptor porphyrins described here, except for Rh**3**,[10] has demonstrated that the geometry around the phosphorus–metal bond does not change significantly between different rhodium and ruthenium porphyrins. It is not clear at this point which factors contribute to these chemical shift effects.

The bpy proton signals show large upfield shifts in the complexes, consistent with being positioned in the shielding region of the Zn–porphyrin. The chemical shifts of $H_n$ and $H_m$ additionally depend on the identity of the porphyrin acceptor in the cage (Figure 3 and Figure 4). In the rhodium cages, $H_n$ and $H_m$ are shifted to the most upfield position for cage **1** ($\delta = 4.49$ and 2.14 ppm, respectively), and are most deshielded in cage **2** ($\delta = 5.43$ and 2.45 ppm, respectively). In the mixture of Rh**5**, Zn**1**, and bpy, the $^1$H NMR spectrum

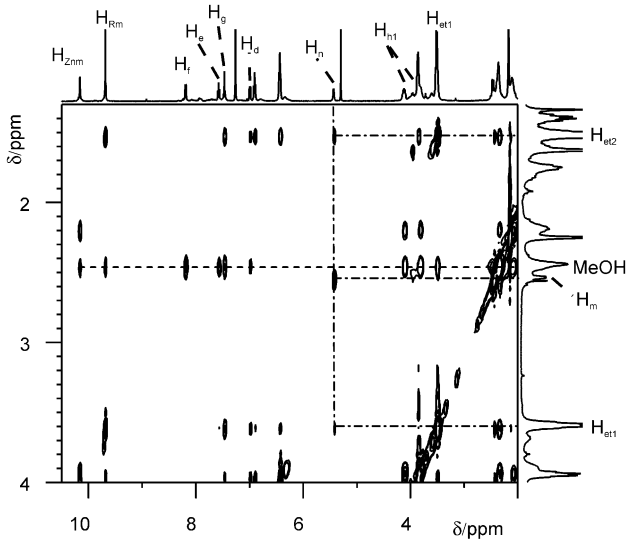


Figure 2. Partial $^1H^1H$ NOESY spectrum of cage **2** showing relevant through-space connectivities. For assignments see text.

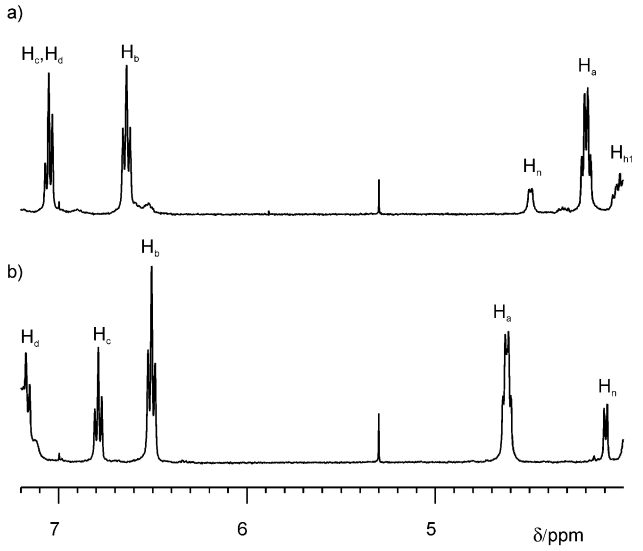


Figure 3. $^1H$ NMR spectra of selected regions of a) cage **1** and b) cage **4**, which show the change in chemical shift of protons a, b, and c.

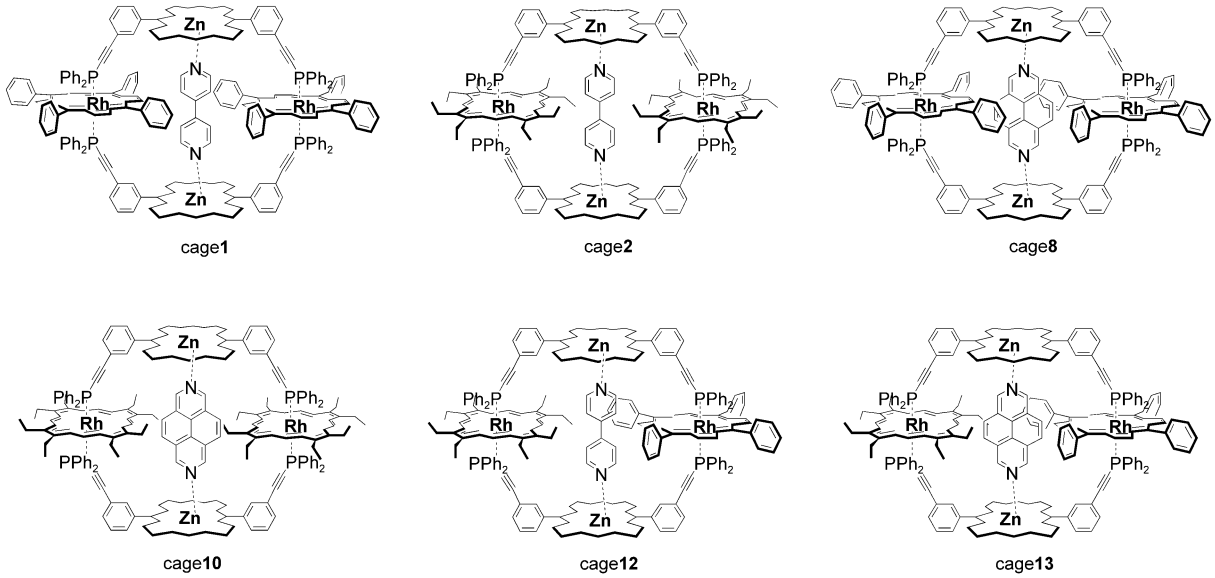


shows a broad signal at approximately 6 ppm for $H_n$; this indicates that bpy is weakly bound to Zn**1** though no cage is formed. A similar pattern is observed in the Ru cages, except that the signals are shifted by 0.2–0.3 ppm upfield compared with the equivalent Rh cage. The fact that cage **1** and cage **4** are the most shielded while cage **2** and cage **5** are the most deshielded suggests that the bpy protons experience additional shielding from the aromatic rings in the *meso* positions of Rh/Ru**2**, not present for Rh/Ru**3**.

**Structural diversity of the template**: The effect of the template structure on the formation of cages was also examined. The study was restricted to the Rh**2** and Rh**3** systems, since these are easier to handle than the Ru systems, and represent the two extremes in terms of steric hindrance of the substituents on the porphyrin acceptors. With Rh**2**, incomplete cage formation was generally observed when templates other than bpy were used. With template **7**, cage **9** was formed in about 80% yield, while for template **6** only 50% of the mixture was transformed into cage **8**. The incomplete formation of these two cage systems is ascribed to the steric requirements of the more bulky templates **6** and **7**.

In cage **9**, two sets of signals are observed for $H_a$, $H_b$, and $H_c$ as a result of restricted rotation of the dimethyl–bpy ligand **7**, the methyl substituents on the bpy rendered the two sides of the cage inequivalent. This effect is not observed for cage **11;** the phenyl groups on the phosphine ligand were equivalent in the $^1H$ NMR spectrum. This indicates that rotation of template **7** is less hindered. The methyl substituent of **7** occurs at around 0 ppm in both cage **9** and cage **11**, and NOEs are observed between this methyl group and the β-pyrrole ethyl side-chains of the acceptor porphyrins; this confirms the close spatial arrangement within the cage. Besides the influence of **7** on the sym-

  

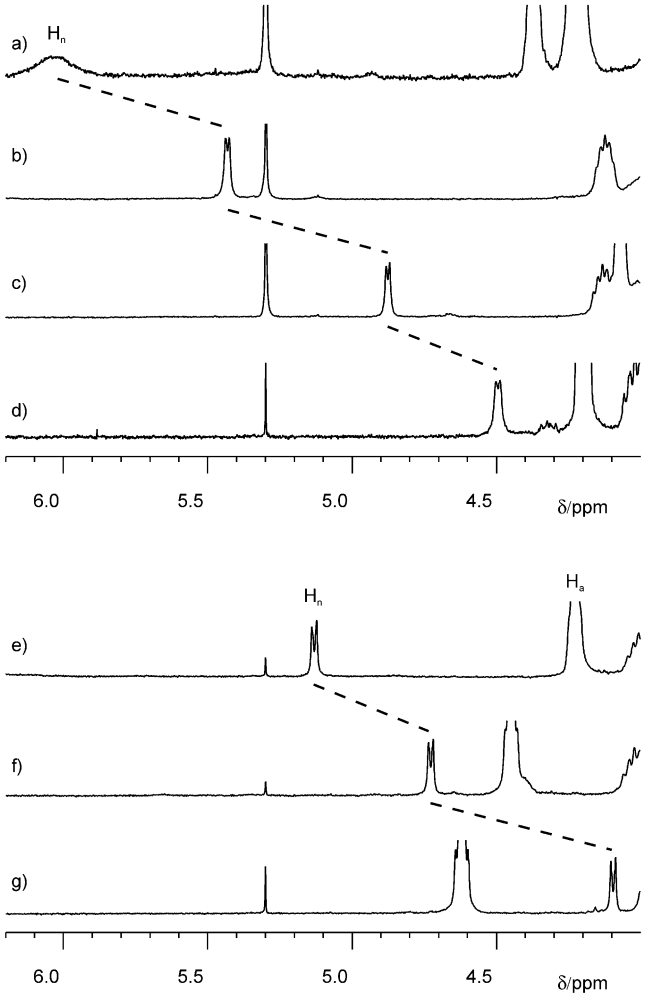


Figure 4. $^1$H NMR spectra of selected regions of a) cage **7**(Rh), b) cage **2**, c) cage **3**, d) cage **1**, e) cage **5**, f) cage **6**, g) cage **4** which show the change in chemical shift of proton n.

metry of cage **9**, the chemical shifts of most of the protons are influenced only marginally by a change in the template. The chemical shifts of $H_a$, $H_b$, and $H_c$ show no difference relative to the equivalent bpy cages. In contrast, the chemical shift of $H_g$ is similar in cage **11** ($\delta = 7.53$ ppm) and cage **2** ($\delta = 7.47$ ppm); however, the chemical shift undergoes a large upfield shift upon binding of **6** into cage **10** ($\delta = 6.61$ ppm; Figure 5). This large change of $\Delta\delta = -0.86$ ppm must take place, because this proton points into the shielding region of **6** in cage **10**. Template **6** also has a small shielding effect on the ethyl side-chains of Rh**3** in cage **10** (Table 2). However, since the porphyrin is rapidly rotating around the P–M–P axis, an average chemical shift is observed between the ethyl side-chains pointing inwards and outwards with respect to the cage. Since the chemical shifts of the ethyl protons is not likely to be strongly influenced by **6** when outside the cage, the ethyl side-chains must be rather close to **6** when inside the cage.

**Formation and stability of the cages**: In order to completely form the cages, the systems require either 24 h at room temperature or a cycle of heating to 65 °C for two minutes, and

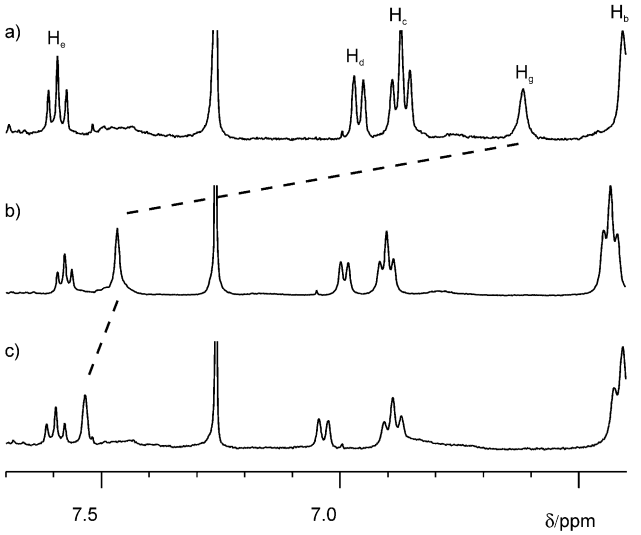


Figure 5. $^1$H NMR spectra of selected regions of a) cage **10**, b) cage **2**, and c) cage **11** which show the change in chemical shift of proton g.

cooling back to room temperature. The formation of the cages by using the latter method could be followed by variable temperature $^1$H NMR spectroscopy. When a mixture of Zn**1**, Rh**2**, and bpy was warmed from room temperature to 45 °C, there was a considerable increase in the amount of cage **1** present. Above 45 °C, the thermodynamic stability is lost, and the mixture completely transforms back into a library. The signal for $H_n$ at $\delta = 4.49$ ppm is not seen in the spectra above 27 °C; this indicates that at elevated temperatures the bpy is outside the cage to a large extent, even though the cyclic porphyrin-complex is intact.

The DCL was also monitored for 12 h at room temperature after addition of bpy (Figure 6). Successive build up and decay of intermediate species is observed in the *meso* proton region of Zn**2** ($\delta \sim 10.3$ ppm), shifted upfield relative to the cage signals. Since the chemical shift of the *meso* protons of Zn**1** are mainly influenced by the presence or absence of any rhodium porphyrin, the upfield shift suggests that the intermediate complexes are composed of various mono- and bisphosphine complexes of the composition [Zn**1**/Rh**2**], [Rh**2**/Zn**1**/Rh**2**] and [Zn**1**/Rh**2**/Zn**1**], with or without a bound bpy group. Given the binding constants of $K_1 = 3 \times 10^7\ \text{M}^{-1}$ for the first binding of phosphine to Rh**2** and $K_2 = 4 \times 10^4\ \text{M}^{-1}$ for the second binding,[6] we can determine that over 99 % of the first binding site has phosphine bound, while 88 % of the second binding site is occupied under the experimental conditions. The depletion of Zn**1** is therefore considered to follow pseudo-first-order kinetics, and the rate constant for the process was determined to be $(2.1 \pm 0.1) \times 10^{-4}\ \text{s}^{-1}$. The cage is rapidly formed at ambient temperatures in comparison with other cages reported in the literature, in which higher temperatures and long reactions times are required for successful formation of the cages.[4,11]

**X-ray crystal structure of [cage 2]$^{2+}$[I]$_2^-$·7 CHCl$_3$**: Single crystals of cage **2** (crystallized as the di-iodide salt [cage **2**]$^{2+}$ [I]$_2^-$·7 CHCl$_3$) were prepared from a stoichiometric (2:2:1) mixture of Zn**1**, [Rh**3**]I and bpy in a chloroform solution

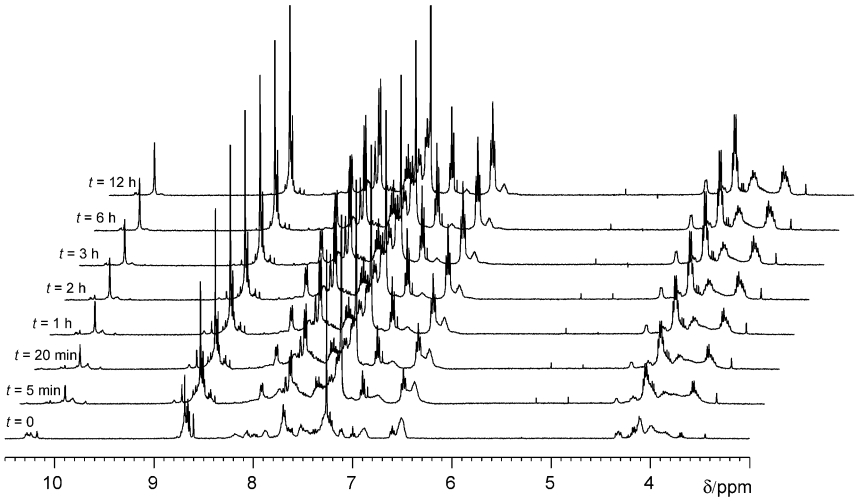


Figure 6. $^1$H NMR spectra of cage **1** after addition of bpy monitored with time.

layered with hexane. The crystals were small and relatively weakly diffracting, and required a synchrotron source for collection of diffraction data suitable for structure solution. The complex crystallizes in space group $P2_1/n$ as a centrosymmetric unit, and displays several notable conformational features. The porphyrin core of Zn**1** adopts a saddle conformation in which the core atoms display an average perpendicular deviation (denoted σ) of 0.190 Å from the least-squares plane defined through all 24 core atoms, and the Zn atom is displaced towards the N atom of the bpy by 0.306 Å from the least-squares plane. The core distortion is somewhat greater than that observed in the closest analogous Zn-diaryl porphyrin, and bears a DPAP group in one *meso* position, and a di-*tert*-butylphenyl group in the opposite *meso* position, for which $\sigma = 0.107$ Å (the crystal structure of Zn**1** itself has not yet been determined). The porphyrin core of Rh**3** deviates considerably less from planarity ($\sigma = 0.086$ Å), comparable to the distortions observed in the isolated di-DPAP complexes of Rh**2**, Rh**4**, and Rh**5**.[10] The angle of the Rh–P bond from the Rh**3** porphyrin least-squares plane (86.7°) is also relative to those observed in the isolated di-DPAP complexes, although the Rh-P distances of 2.356(1) Å are slightly shorter (cf. 2.371(1), 2.369(1), and 2.369(1) Å in [Rh**2**(dpap)$_2$], [Rh**4**(dpap)$_2$], and [Rh**5**(dpap)$_2$], respectively).[10]

To accommodate the bpy template effectively within the cage cavity, the overall geometry of the cage deviates considerably from the ideal conceptual "box" represented in Scheme 1. Projection approximately along the cross-cage Zn···Zn vector reveals that the 5,15-axes of the Zn**1** porphyrins are rotated by about 10° from the plane passing through all four metal atoms (Figure 7a). To accommodate this twist, the dihedral angles formed between the *meso*-phenyl groups and the least-squares plane of Zn**1** differ significantly, one being close to perpendicular (84.3(1)°), and the second deviating considerably from it (70.9(2)°). This substantial distortion of the cage geometry is in accordance with our previous suggestions, derived from $^1$H NMR data.[6] Projection approximately along the Rh···Rh vector (Figure 7b) shows that the least-squares planes through the Rh**3** porphyrins are tilted by 60.1(1)° with respect to the planes through the Zn**1** porphyrins. The perpendicular separation between the least-squares planes of the Zn**1** porphyrins is about 11.55 Å, and the two porphyrins are offset from each other, such that the bpy ligand is tilted by about 17° from the normal to the Zn**1** porphyrin planes. The Zn-N distances of 2.201(4) Å are relative to those in pyridyl complexes of other Zn porphyrins. Projection onto the plane, that contains four metal atoms (Figure 7c), reveals that the Rh**3** porphyrins adopt angles of

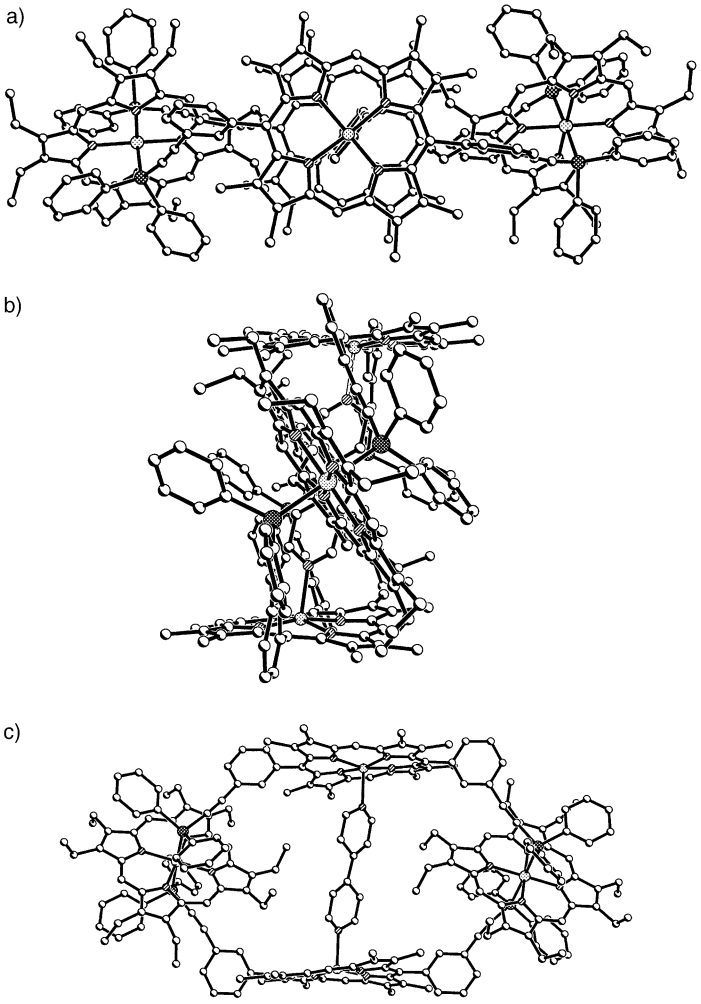


Figure 7. Centrosymmetric cage **2** moiety from the crystal structure of [cage **2**]$^{2+}$[I]$_2^-$·7 $CHCl_3$ (H atoms and hexyl side chains on Zn**1** omitted), a) projected along the cross-cage Zn···Zn vector, b) projected along the cross-cage Rh···Rh vector, and c) projected onto the plane containing all four metal atoms.

  

rotation about the P–Rh–P axes that brings the acetylenic groups of the DPAP moieties approximately over the unsubstituted *meso* positions; a conformation similar to that observed in isolated [Rh**4**(dpap)$_2$].[10] This rotation brings two ethyl substituents in β-pyrrole positions into close proximity with the bpy template in the cage cavity, consistent with the observed NOEs between the bpy protons ($H_m$ and $H_n$) and the ethyl side chains on Rh**3** ($H_{et1}$ and $H_{et2}$) in solution. The bpy substituent displays orientational disorder about the Zn···Zn axis (modelled in two closely related orientations), consistent with the observation of the rapid rotation of bpy (and also template **6**) within the cage cavity in solution.

**Complex mixtures**: To evaluate the scope of the system, we examined the selectivity of the templates for the formation of one specific cage from complex mixtures. Those DCLs were prepared by mixing different rhodium or ruthenium porphyrins with Zn**1**, and, after addition of various templates, the DCLs were examined by $^1$H NMR spectroscopy. As a first observation, we found that it was necessary to have sufficient amounts of each building block for complete formation of all possible cages. Without sufficient template or Zn**1**, the Rh/Ru porphyrins compete for the template through metal–nitrogen complexation, and interfere with cage formation.

**Mixture 1**: This mixture was prepared from Zn**1**, Rh**2**, Rh**3** and **6** in the ratio 2:1:1:1. From the experiments described above, we expected that in this system cage **10** should form preferentially. The final $^1$H NMR spectrum observed corresponded to the superposition of several spectra, which were attributable to the spectra of cage **8**, cage **10**, and the mixed cage **13**. The signals for $H_{Znm}$ at 10.23 ppm and $H_k$ at 3.03 ppm, which appear in-between the resonances for cage **8** and cage **10**, are assigned to the mixed cage **13**. By contrast, the chemical shifts for the porphyrin protons $H_\beta$ and $H_{Rm}$, and the phosphorus phenyl substituents $H_a$, $H_b$, and $H_c$ are insensitive to the overall composition of the cage. The ratio of the cages was not statistical with cage **10** comprising 40%, cage **13** comprising 20%, and cage **8** comprising 12% of the mixture; the rest of the building blocks remained in dynamic equilibrium, as seen in the appearance of some broad signals. Although cage **10** is indeed the preferred cage, the templating effect of **6** is not sufficient to specifically select cage **10** from the complex mixture.

**Mixture 2**: A mixture of Zn**1**, Rh**5**, Rh**3**, and bpy in the ratio 2:1:1:1 was studied next. Since Rh**5** does not form a cage with bpy in isolation, no cage that incorporates Rh**5** should be observed, and cage **2** should be formed exclusively. On titration of bpy into the DCL, a superposition of the two expected spectra for cage **2** and the DCL formed from the remaining building blocks is observed. The signal for $H_n$ bound to Zn**1** and one sharp $H_{Znm}$ signal integrate to 50% of the total for $H_{Znm}$, which corresponds to cage **2**. The remaining small signals in the spectrum, indicate that no mixed cage is observed. Thus, as expected from the individual DCLs, the selection and amplification of cage **2** from this complex mixture is virtually complete.

**Mixture 3**: The DCL was prepared from Zn**1**, Rh**2**, and Rh**3** in a 2:1:1 ratio (Figure 8). On titration of the required amount of bpy into the solution, the formation of three cages is observed: cage **1**, cage**2**, and a mixed cage **12**. The cages are formed in the ratio 0.16:1:0.58, with $^1$H NMR signals for $H_n$ at $\delta = 4.49$, 5.43 and 5.16 ppm, respectively. The resonance for the bpy proton $H_n$ in cage **12** is not exactly halfway between those for cage **1** and cage **2**, but is shifted by 0.2 ppm downfield towards the signal that corresponds to cage **2**. The fact that the electronic effects of the porphyrins Rh**2** and Rh**3** are not superimposable when combined in a cage complex, suggests that, the geometry of cage **12** is not simply an average of cage **1** and cage **2**. Clearly, not all of the Rh**2** present in the mixture is used for cage formation, since the expected statistical ratio of 1:2:1, or even a 1:1 for-

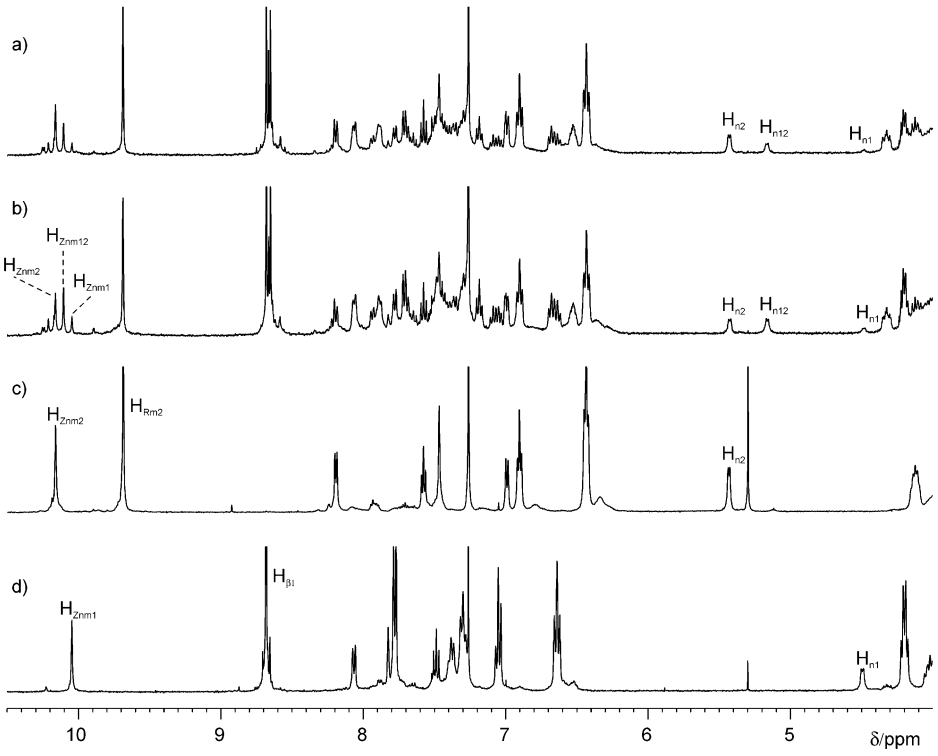


Figure 8. $^1$H NMR spectra of a) mixture **3** (containing cage **2**, cage **1** and cage **12**) at $t = 0$ min, b) mixture **3** at $t = 4$ days, c) cage **2**, d) cage **1**.

mation of cage **1** and cage **2**, is not observed. Cage **1** appears to be disfavoured and kinetically more labile than the other cages, as judged from its broader signal for $H_n$. A variable temperature $^1$H NMR study showed that this signal disappeared upon heating to 35 °C, which indicates that the bpy is in more rapid exchange with free species in cage **1** than in either cage **2** or cage **12**. $H_{Rm}$ of the Rh**3** porphyrin appears as a singlet, while $H_\beta$ for the Rh**2** porphyrin appears as three different signals, which corresponds to cage **1**, cage **12**, and the remaining porphyrin which is not part of a cage NOESY experiments performed on this mixture resulted in exchange peaks between all three $H_n$ signals for the three different cages, which showed that the bpy is exchanging between the cages, and that the mixture, as a whole, remains dynamic. The relative amounts of the three cages were found to alter with time, being 0.36:1:1.07 (cage **1**:cage **2**:cage **12**) after four days: the relative amounts of cage **1** and cage **12** increase at the expense of cage **2**. After four days, no further change in the composition was observed. Thus, the initial ratio, formed upon cooling the mixture from 65 °C to 25 °C during the annealing process, represents the kinetic distribution, in which cage **2** initially appears to be favoured. After four days, the thermodynamic equilibrium is reached, which contains a greater proportion of cage **1** and cage **12**. To rule out the possibility that cage **1** dissociates at lower concentrations, which could explain the smaller amount of cage **1** present, a series of dilution experiments was performed on cages **1** and **2** to test the relative stabilities of the cages. Between the concentrations of $2.14\times10^{-3}$ and $1.79\times10^{-4}$ molL$^{-1}$, there was no significant change in composition of the cage as expected from the estimated stability constant of $\sim10^{40}$ M$^{-1}$ of the cages.

**Mixture 4**: The final mixture examined was the most complex, which involves Zn**1**, Rh**2**, Rh**3**, **6**, and bpy in the ratio 4:2:2:1:1. On titrating **6** and bpy into the mixture, all possible cages are formed with the expected initial preference for cage **2** and cage **10**. Two $H_{Rm}$ signals are observed for Rh**3**, that correspond to the two cages formed with the templates bpy and **6**. Multiple signals are observed for the $H_\beta$ protons at 8.68, 8.67, and 8.65 ppm which are associated with cage **1**, cage **8**, cage **12**, cage **13**, and Rh**1** not bound within a cage. More than six signals are observed for the $H_{Znm}$ protons that correspond to the six possible cages and to incomplete formation of the cage with Rh**1** and **6** (Table 3). Initially, the

Table 3. Selected $^1$H NMR chemical shift data [$\delta$] for the mixed cages.

| | cage **1** | cage **2** | cage **12** | cage **8** | cage **10** | cage **13** |
|---|---|---|---|---|---|---|
| Znm | 10.05 | 10.16 | 10.11 | 10.11 | 10.28 | 10.23 |
| n | 4.49 | 5.43 | 5.16 | | | |
| k | | | | 2.94 | 3.20 | 3.05 |

cages were formed in the ratio 1:0.71:0.25:1.97:0.97 for cage **2**:cage **12**:cage **1**:cage **10**:cage **13** (the amount of cage **8** cannot be determined since the signal is obscured). After four days, the relative signal intensities had changed to give a final ratio of 1:1.35:0.44:1.60:1.23, that corresponds to increased amounts of cage **12**, cage **1** and cage **13** (as observed for mixture 3). This confirms that although the cages are thermodynamically stable, their kinetic lability allows the system to equilibrate, and hence, reach final thermodynamic distribution after several days. Since the cage composed of Rh**2** and **6** (cage **8**) has limited stability, it might have been expected that the mixture would give rise only to cage **1** and cage **10**. However, this is not the case, and all possible combinations are observed. Thus, it has not been possible to select and amplify any specific cage from this complex mixture. The initial preference of the system for cages involving Rh**3** probably arises as a result of the lesser steric hindrance of Rh**3** compared to Rh**2**. The ability of the system to form the mixed cage **13** suggests that this cage also has enhanced stability compared with cage **8**.

## Conclusion

In this study, we have enlarged the structural diversity in cyclic tetraporphyrin cages. Both rhodium(III) and ruthenium(II) porphyrins have been incorporated, and the homoporphyrinic cages (with respect to the Ru or Rh porphyrin) can be selected and amplified from dynamic combinatorial libraries by using various ligands as templates. In general, the rhodium cages are easier to handle, because of the inherent problems of removing the carbonyl ligand from ruthenium porphyrins. In addition, the $^1$H NMR spectra obtained with rhodium porphyrins are usually better resolved than those of their ruthenium counterparts. The absolute amount of amplification from the DCLs is strongly dependent on the combination of the Ru/Rh porphyrin and the template: the more sterically demanding the porphyrin, the smaller the template should be to obtain virtually complete amplification. In the case of Ru/Rh**5**, which bears bulky tertiary butyl groups on the *meso* phenyl substituents, cages are not formed at all. The largest template **6** forms cages quantitatively only with Rh/Ru**3**, the least sterically demanding porphyrin.

$^1$H NMR spectroscopy reveals that the chemical shifts of several characteristic protons, that is, $H_g$ and $H_{a-c}$, show large differences upon changing the identity of the acceptor porphyrin and the central metal. These chemical shift differences are unlikely to arise only from variation in the geometry around the rhodium or ruthenium metal centre, since these are too small to account for the observed variations. The large differences in the shielding of the characteristic protons are most likely to arise from variations in the geometry of the cages, in combination with variable ring current effects that depend on the identity of the central metal in the acceptor porphyrins. The X-ray crystal structure of cage **2** demonstrates that the cages can adopt severely distorted conformations to accommodate the relatively short template bpy.

An extension to mixed DCLs showed that only limited selectivity is displayed by the various templates. Formation of mixed cages that contain two different rhodium porphyrins prevents effective selection, although the kinetic lability of the systems allows for some amplification. This lability, however, also prevents isolation of the cages. Effective am-

  

plification can only be achieved if the system is biased in such a way that some of the porphyrins used are inherently unable to form cages, that is, Ru/Rh**5**.

## Experimental Section

All porphyrins were prepared following literature procedures[12,13] from either pyrrole and the appropriate aldehyde refluxed in propanoic acid, or dipyrromethane and the appropriate aldehyde in TFA-methanol. Octaethyl porphyrin was used as purchased from Acros. Zn**1** was prepared from the reaction of the *meta*-bis(acetylene)porphyrin with $ClPPh_2$ under anaerobic and water free conditions following the literature synthesis.[9] Ruthenium was inserted by using standard ruthenium insertion conditions; triruthenium dodecacarbonyl and the required porphyrin were heated in decalin for 48 h to give the ruthenium porphyrin.[13] Rhodium porphyrins were prepared according to the literature procedure[14] by stirring the porphyrin and $Rh(CO)_4Cl_2$ with NaOAc in anaerobic conditions for four hours, and then $I_2$ was added to give the iodo porphyrin. Bpy was used as purchased from Aldrich. Templates **6** and **7** were prepared by following literature procedures.[15,16]

Cages were formed as NMR samples in $CDCl_3$ by combining the components, either by heating to 65 °C and appling a cooling cycle, or by leaving the solutions to equilibrate for 24 h.[5] In all experiments, Zn**2** (2.00 mg, 1.50 μmol) was dissolved in $CDCl_3$ (200 μL) in a degassed NMR tube, fitted with a rubber septum; the acceptor-porphyrins (1.50 μmol in 200 μL $CDCl_3$) and the templates (0.75 μmol in 20 μL $CDCl_3$) were added by using a syringe, and the solvent was adjusted to 600 μL. NMR spectra were then recorded. In the case of the ruthenium-containing cages, the DCLs were prepared as follows: the ruthenium porphyrins and Zn**1** were mixed in equimolar amounts in $CHCl_3$, and the solvent was removed under reduced pressure. The mixture was redissolved, and the procedure was repeated twice to completely remove the carbonyl. The mixture was finally taken up in $CDCl_3$ and used for the formation of the cages.

$^1$H NMR measurements were performed in $CDCl_3$ at 300 K (unless otherwise stated) by using either a Bruker DRX500 or a Bruker DPX400. The 2D spectra for mixture **4** were collected on a 500 MHz Bruker DRX fitted with a cryoprobe.

Single-crystal X-ray diffraction data for $[\text{cage}\,\mathbf{2}]^{2+}\cdot 2I^-\cdot 7CHCl_3$ were collected at Station 9.8, Daresbury SRS, by using a Bruker SMART diffractometer equipped with a PROTEUM200 CCD detector. Two of the four independent hexyl chains were disordered and modelled in two equally occupied orientations, and all hexyl chains were refined with restrained geometry and isotropic displacement parameters common to carbon atoms at equivalent positions C2–C6 along each chain (five independent parameters in total). The bpy moiety was also disordered and refined in two equally occupied orientations with restrained geometries. Five independent chloroform solvent molecules were located and refined with restrained geometries, three with full site occupancy, and two with 25% site occupancy (summing to seven $CHCl_3$ molecules per centrosymmetric cage).

Crystal data for $[\text{cage}\,\mathbf{2}]^{2+}\cdot 2I^-\cdot 7CHCl_3$: $C_{265}H_{291}Cl_{21}I_2N_{18}P_4Rh_2Zn_2$, FW = 5186.85, $T = 150$(2 K, synchrotron radiation $\lambda = 0.6850$ Å, red plate $0.25 \times 0.18 \times 0.02$ mm, space group $P2_1/n$, $Z = 2$, $a = 25.1838(9)$, $b = 16.5456(6)$, $c = 32.5020(11)$ Å, $\beta = 93.902(2)°$, $V = 13511.6(8)$ Å$^3$, $\rho_{calc} = 1.275$ gcm$^{-3}$, $\mu = 0.808$ mm$^{-1}$, $3.39 < \theta < 25.35°$, 68284 total data, 26878 unique data ($R_{int} = 0.0426$), $R1$ $[I > 2\sigma(I)] = 0.0804$, $wR2 = 0.2545$, $S = 1.03$.

CCDC-213358 contains the supplementary crystallographic data for this paper. These data can be obtained free of charge via www.ccdc.cam.ac.uk/conts/retrieving.html (or from the Cambridge Crystallographic Data Centre, 12 Union Road, Cambridge CB2 1EZ, UK; fax: (+44) 1223–336–033; or e-mail: deposit@ccdc.cam.ac.uk).

## Acknowledgement

Financial support from the Swiss National Science Foundation (E.S.) and from the EPSRC is gratefully acknowledged.

[1] a) S. Otto, R. L. E. Furlan, J. K. M. Sanders, *Drug Discovery Today* **2002**, *7*, 117–125; b) S. Otto, R. L. E. Furlan, J. K. M. Sanders, *Curr. Opin. Chem. Biol.* **2002**, *6*, 321–327; c) J.-M. Lehn, A. V. Eliseev, *Science* **2001**, *291*, 2331–2332.

[2] Some examples are: a) B. Brisig, J. K. M. Sanders, S. Otto, *Angew. Chem.* **2003**, *115*, 1308–1311; *Angew. Chem. Int. Ed.* **2003**, *42*, 1270–1273; b) G. R. L. Cousins, R. L. E. Furlan, Y.-F. Ng, J. E. Redman, J. K. M. Sanders, *Angew. Chem.* **2001**, *113*, 437–442; *Angew. Chem. Int. Ed.* **2001**, *40*, 423–428; c) A. V. Eliseev, M. I. Nelen, *Chem. Eur. J.* **1998**, *4*, 825–834; d) V. A. Polakov, M. I. Nelen, N. Nasarpack-Kandlousy, A. D. Ryabov, A. V. Eliseev, *J. Phys. Org. Chem.* **1999**, *12*, 357–363; e) S. L. Roberts, R. L. E. Furlan, S. Otto, J. K. M. Sanders, *Org. Biomol. Chem.* **2003**, *1*, 1625.

[3] a) M. Crego Calama, P. Timmerman, D. N. Reinhoudt, *Angew. Chem.* **2000**, *112*, 771–774; *Angew. Chem. Int. Ed.* **2000**, *39*, 755–758; b) J. M. Rivera, S. L. Craig, T. Martin, J. Rebek, Jr., *Angew. Chem.* **2000**, *112*, 2214–2216; *Angew. Chem. Int. Ed.* **2000**, *39*, 2130–2132; c) Y. Ma, S. V. Kolotuchin, S. C. Zimmerman, *J. Am. Chem. Soc.* **2002**, *124*, 13757–13769.

[4] a) I. Huc, M. J. Krische, D. P. Funeriu, J.-M. Lehn, *Eur. J. Inorg. Chem.* **1999**, 1415–1420; b) D. M. Epstein, S. Choudhary, M. Rowen Churchill, K. M. Keil, A. V. Eliseev, J. R. Morrow, *Inorg. Chem.* **2001**, *40*, 1591–1596; c) F. M. Tabellion, S. R. Seidel, A. M. Arif, P. J. Stang, *Angew. Chem.* **2001**, *113*, 1577–1580; *Angew. Chem. Int. Ed.* **2001**, *40*, 1529–1532; d) M. Albrecht, O. Blau, R. Fröhlich, *Chem. Eur. J.* **1999**, *5*, 48–56; e) M. Ziegler, J. J. Miranda, U. N. Andersen, D. W. Johnson, J. A. Leary, K. N. Raymond, *Angew. Chem.* **2001**, *113*, 755–758; *Angew. Chem. Int. Ed.* **2001**, *40*, 733–736; f) S. Hiraoka, M. Fujita, *J. Am. Chem. Soc.* **1999**, *121*, 10239–10240; g) E. C. Constable, G. E. Housecroft, T. Kulke, C. Lazzarini, E. R. Schofield, Y. Zimmermann, *J. Chem. Soc. Dalton Trans.* **2001**, 2864–2871.

[5] E. Stulz, Y.-F. Ng, S. M. Scott, J. K. M. Sanders, *Chem. Commun.* **2002**, 524–525.

[6] E. Stulz, S. M. Scott, A. D. Bond, Otto, S. , J. K. M. Sanders, *Inorg. Chem.* **2003**, *42*, 3086–3096.

[7] a) E. Stulz, M. Maue, N. Feeder, S. J. Teat, Y.-F. Ng, A. D. Bond, S. L. Darling, J. K. M. Sanders, *Inorg. Chem.* **2002**, *41*, 5255–5268; b) E. Stulz, J. K. M. Sanders, M. Montalti, L. Prodi, N. Zaccheroni, F. de Biani, E. Grigiotti, P. Zanello, *Inorg. Chem.* **2002**, *41*, 5269–5275.

[8] a) H.-J. Kim, N. Bampos, J. K. M. Sanders, *J. Am. Chem. Soc.* **1999**, *121*, 8120–8121; b) B. G. Maiya, N. Bampos, A. A. Kumar, N. Feeder, J. K. M. Sanders, *New J. Chem.* **2001**, *25*, 797–800; c) J. E. Redman, N. Feeder, S. J. Teat, J. K. M. Sanders, *Inorg. Chem.* **2001**, *40*, 2486–2499.

[9] S. L. Darling, E. Stulz, N. Feeder, N. Bampos, J. K. M. Sanders, *New J. Chem.* **2000**, *24*, 261–264.

[10] These results will be reported elsewhere.

[11] a) D. W. Johnson, K. N. Raymond, *Inorg. Chem.* **2001**, *40*, 5157–5161; b) D. L. Caulder, R. E. Powers, T. N. Parac, K. N. Raymond, *Angew. Chem.* **1998**, *110*, 1940–1943; *Angew. Chem. Int. Ed.* **1998**, *37*, 1840–1843.

[12] A. D. Adler, F. R. Longo, J. D. Finarelli, J. Goldmaker, J. Assour, L. Korsakoff, *J. Org. Chem.* **1967**, *32*, 476.

[13] V. Marvaud, A. Vidal-Ferran, S. J. Webb, J. K. M. Sanders, *J. Chem. Soc. Dalton Trans.* **1997**, 985–990.

[14] H.-J. Kim, J. E. Redman, M. Nakash, N. Feeder, S. J. Teat, J. K. M. Sanders, *Inorg. Chem.* **1999**, *38*, 5178–5183.

[15] a) E. F. Lier, S. Hünig, H. Quast, *Angew. Chem.* **1968**, *80*, 343–352; *Angew. Chem. Int. Ed. Engl.* **1968**, *7*, 814; b) J. E. Redman, Ph.D. thesis, University of Cambridge **2001**.

[16] J. Rebek, Jr, T. Costello, R. Wattley, *J. Am. Chem. Soc.* **1985**, *107*, 7487–7493.

Received: June 24, 2003 [F5265]